*Acta Geologica Polonica*, Vol. 75 (2025), No. 4, e61
DOI: 10.24425/agp.2025.157026

# The impact of water inundation on the geotechnical behaviour of artificial soil made from waste materials: contrasting results in total and effective stress analysis

TOMASZ SZCZEPAŃSKI[1], ŁUKASZ KRYSIAK[2], KAMIL KIEŁBASIŃSKI[1]* and ŁUKASZ KACZMAREK[2]

[1] *University of Warsaw, Faculty of Geology, Żwirki i Wigury 93, 02-089 Warszawa, Poland;*
*e-mails: tomasz.szczepanski@uw.edu.pl; k.kielbasinski@uw.edu.pl*
[2] *Warsaw University of Technology, Faculty of Building Services, Hydro and Environmental Engineering, Nowowiejska 20, 00-653 Warszawa, Poland;*
*e-mails: lukasz.krysiak@pw.edu.pl; lukasz.kaczmarek@pw.edu.pl*
** Corresponding author*

ABSTRACT:

Szczepański, T., Krysiak, Ł., Kiełbasiński, K. and Kaczmarek, Ł. 2025. The impact of water inundation on the geotechnical behaviour of artificial soil made from waste materials: contrasting results in total and effective stress analysis. *Acta Geologica Polonica*, **75** (4), e61.

Applying new waste-derived soils to engineering causes challenges related to their specific properties. Colliery spoils and fluidized bed combustion ash used in embankments are particularly sensitive to variation in water content. In this paper, triaxial compression (TRX) and bender element tests (BET) were conducted on compacted samples of spoil-ash mixtures under confining stress (0–500 kPa). Two water contents were assumed, i.e., 'natural (14.6%) and 'wet', after 36 h inundation (20–25%). The purpose was to observe the impact of a one-time water ingress on mechanical properties. The results are ambiguous and depend on the interpretation of the approach. The first approach is typical for rock testing, with the UC test used to define strength. No pore water pressure measurement is made in this approach; the results are based on total stress analysis (TSA). The second method is characteristic for soil mechanics effective stress analysis (ESA), where pore water pressure is considered; it uses TRX with appropriate sample saturation. This paper attempts a combined approach and compares the results depending on which interpretation is used. With TSA, water inundation seems to have significantly affected the tested samples (reduction of cohesion by up to 89% and initial shear modulus by up to 41%), whereas ESA reveals a much smaller effect (a drop by up to 55% and 20%, respectively). A simple numerical analysis (Finite Element Method) illustrates the observed change in mechanical properties, with the slope stability safety factor being reduced five-fold or two-fold (TSA and ESA, respectively).

**Key words:** Colliery spoils; Fluidized bed combustion ash; Water content; Bender element test; Total stress; Effective stress; Triaxial compression; Unsaturated soil.

## INTRODUCTION

Current challenges related to anthropogenic pressure on the environment have led to a steady increase in the amount and variety of man-made alternative materials (often wastes) used in civil engineering, including many substitutes for natural aggregates (Kozioł and Baic 2019; Głuchowski *et al.* 2020; Bisht 2022; Gabryś *et al.* 2023). The benefits of using industrial by-products include low cost, resource preservation, and reduced waste landfilling. A mixture of colliery spoils (waste stone, mine tailings) and

fluidized bed combustion (FBC) bottom ash is one example of a new man-made soil that has been utilized in geotechnical engineering in Poland for over ten years (Szymkiewicz *et al.* 2012). Introducing new materials into construction carries a risk due to their properties not being fully recognised. In the case of the above-mentioned mixture the risk takes the form of excessive swelling (Krysiak *et al.* 2023). The material is particularly interesting as a mixture of two distinct industrial by-products acting as alternatives to traditional materials (aggregate + binder). The first component of the mixture, colliery spoil, a by-product of hard coal mining, has a relatively long history of application in civil engineering in embankments (Kettle 1983; Laan *et al.* 1984; Rainbow *et al.* 1987; Skarżyńska 1995b). Besides some generally beneficial properties, it is also exceptionally heterogeneous, has a variable mineral composition, high water content, is susceptible to grain disintegration, spontaneous combustion and pollutant leaching (Kettle 1983; Skarżyńska 1995a; Cadierno *et al.* 2014; Suescum-Morales *et al.* 2019). The second component, FBC bottom ash, a by-product of fluidized bed combustion of hard coal, has limited use in civil engineering (Gazdič *et al.* 2017; Zahedi and Rajabipour 2019). Its application potential and properties have been discussed by Yoon *et al.* (2007) and Ohenoja *et al.* (2020)

One way to address the previously-mentioned adverse properties of raw colliery spoil is to use a binder, such as Portland cement (Pilecka and Morman 2017) or hard coal fly ash (also FBC ash; Gruchot 2014). The benefits include increased load capacity, reduced permeability, solubility, and swelling (Szymkiewicz *et al.* 2012). That paper reported full-scale applications of the material in levees and road embankments in Poland based on a technical approval certificate (IBDiM 2010). At the same time, similar use of raw, unmixed colliery spoil requires certain precautions, including superficial sealing layers due to the material's proneness to weathering (Borys *et al.* 2002). This raises questions regarding potentially similar problems in the spoil-ash mixtures. Gruchot and Zydroń (2019) stated their usefulness for embankment construction, noting that a potential drop in cohesion would drastically decrease the factor of safety regarding slope stability.

The working conditions of embankments should typically provide a certain period when the mixed and compacted reactive material undergoes chemical binding before it is subjected to external water inflow or saturation. In such a scenario, the mechanical properties of the built-in spoil-ash mixture should gradually increase as the binding progresses in relatively stable conditions. Then, due to sudden wetting or saturation, some of its properties might change permanently or temporarily (and repetitively). The research on the spoil-ash mixture by Szymkiewicz *et al.* (2012) included its inundation in water for 4–15 days, hinting at the related risks. It was not specified, however, if the mixture was left to cure before submersion.

The relationship between the water content and the mechanical properties of soils has long been, and still is, an essential area of research. Besides embankment safety, it plays a significant role in the better understanding of, e.g., the occurrence of landslides after rainfall (Wei *et al.* 2019) or in foundation design (Feng *et al.* 2023). The most common approach is to test undisturbed (or reconstituted) soil samples with various imposed water content in direct shear (Gruchot *et al.* 2020), triaxial compression (TRX, e.g., Mouazen *et al.* 2002) or uniaxial compression in case of rocks (Babets *et al.* 2020). Attempts to establish the relationship between water content and soil shear strength may yield somewhat differing results, as the dependency is also influenced by the bulk density/degree of compaction or the imposed stress (Mouazen *et al.* 2002; Feng *et al.* 2023). A recent comprehensive study on cohesive soils (Gong *et al.* 2022) indicated a clear negative relationship between water content and internal friction angle ($\varphi$), as well as cohesion ($c$), thus strongly affecting shear strength. Mouazen *et al.* (2002) cited other reports on the water-shear strength relation in cohesive soils, some of which suggested the existence of a peak cohesion value for a particular moisture content (Rajaram and Erbach 1997). Their original research on the shear strength of sandy loam soil points to a linear decrease in $c$ with increasing water content, while $\varphi$ is unaffected. A similar conclusion is found in Feng *et al.* (2023), but $\varphi$ was also negatively related, though less strongly than $c$.

Investigating waste-derived, man-made soils is particularly important because, besides the physical phenomena typical for natural soils, they exhibit other properties, e.g., high proneness to weathering and grain disintegration. Chemical reactivity in contact with water is also typical, which might lead to crystallization, swelling, leaching, etc. An ash-slag mixture from a landfill shows a 30–43% decrease in $c$ and 4–6% in $\varphi$ in a water-saturated state (Gruchot *et al.* 2020); a recycled aggregate of similar origin underwent a reduction in $c$ of approximately 60%, while $\varphi$ was not significantly affected (Zawisza and Gruchot 2017).

The bender element test (BET) is a comparatively recent non-destructive method for testing selected

mechanical properties of soils. Employing mechanical waves (S-waves and P-waves) allows the assessment of changes in the material's structure, e.g., caused by freeze-thaw cycles (Jafari and Lajevardi 2022). BET enables the determination of the small strain shear modulus ($G_0$) under different imposed stresses, e.g., in the TRX chamber. Kim *et al.* (2021) used BET to investigate the role of the degree of saturation on the small strain properties of fine sand. Their results suggest that the increasing water content is generally related to a greater Poisson's ratio ($v$) and a decrease in wave travel velocity. Full saturation, however, has a particularly significant effect in the form of a sharp increase in P-wave velocity and a $v$ value of 0.5. An interesting part of the research presented by Kim *et al.* (2021) also proves that BET is sensitive to the average degree of sample saturation and its volumetric distribution, as well as the orientation of layers.

This paper aims to investigate the effect of a sudden water content increase on selected properties of a hardened aggregate-binder mixture of colliery spoil and FBC bottom ash. Laboratory-made mixture samples after 60 days of curing, in a state of 'natural' water content or after water saturation, were tested using the BET and TRX methods. Shear wave velocity ($V_s$), and resulting shear modulus ($G_0$), angle of internal friction ($\varphi$), and cohesion ($c$) were estimated, both in air-dry and wet states. The aims of the study arise from the need to expand the understanding of the material's behaviour in actual working conditions and the related risks, to present a multi-method approach when investigating the relationship between water content and mechanical properties, and to present the above in the context of a different approach to the interpretation, that is total (TSA) and effective (ESA) stress analysis.

## MATERIAL AND METHODS

### Material properties and sample preparation

The first component of the mixture, colliery spoil, originated from the Sobieski Coal Mine in Jaworzno, Poland. It was collected directly after a wet coal extraction process in a mechanical coal enrichment plant and thus had an elevated original water content. The second component is FBC bottom ash from the combustion of hard coal and coal sludge in a circulating fluidized bed boiler. It was obtained from the Jaworzno II Power Plant in a dry-cooled state. Potable water was added to the mixture to reach the desired water content. Selected properties of the two raw materials are presented in Table 1 and Text-fig. 1. Additional information on the raw materials can be found in Krysiak *et al.* (2023).

A single mixture composition was assumed in the tests based on previous studies (Krysiak 2022; Krysiak *et al.* 2023; Table 2). For comparison, the composition of an analogous mixture approved for use in engineering structures in Poland is also included (Szymkiewicz *et al.* 2012). The two mixture compositions are similar, ensuring effective compaction and a strong stabilizing effect through the binding (hydration) of the bottom ash.

The experiment consisted of the testing of cylindrical samples of the hardened mixture, 140 mm in height and 69 mm in diameter. Preparation by drilling and cutting from a larger mass is difficult due to the material's brittleness (water-assisted drilling is also not acceptable in the context of the aim of the research). Thus, a modified rammer-compaction method was assumed for sample preparation, roughly based on PN-EN 13286-50 (CEN 2004), but using non-standard discarded moulds. The original max-

| Property | Colliery spoils | Bottom ash | Test method |
|---|---|---|---|
| Particle size distribution | 0-31.5 mm (mGr) | 0-4 mm (mSa) | PN-B-04481:1988 (PKN 1988)(sieve analysis) |
| Natural water content | ~16.5% (equal to water absorption) | 0% | PN-EN 1097-6 (PKN 2022) / PN-EN ISO 17892-1 (PKN 2017) |
| Oven-dried particle density | 1.62 g/cm$^3$ | 2.70 g/cm$^3$ | PN-EN 1097-6 (PKN 2022) / PN-EN 1097-7 (PKN 2008) |
| Saturated and surface-dried particle density | 1.89 g/cm$^3$ | N/A | PN-EN 1097-6 (PKN 2022) |

Table 1. Selected properties of the raw components of the mixtures.

| | Colliery spoils (dry wt.) [kg] | Bottom ash [kg] | Water [kg] | Water content [%] |
|---|---|---|---|---|
| Tested mixture | 1.000 | 0.271 | 0.210 | 16.5 |
| Exemplary mixture approved for construction (Szymkiewicz *et al.* 2012) | 1.000 | 0.250 | 0.206 | 16.5 |

Table 2. Composition of the test samples of the mixtures (per 1 kg of colliery spoils). Composition of a similar material approved for the construction of embankments in Poland included for comparison.

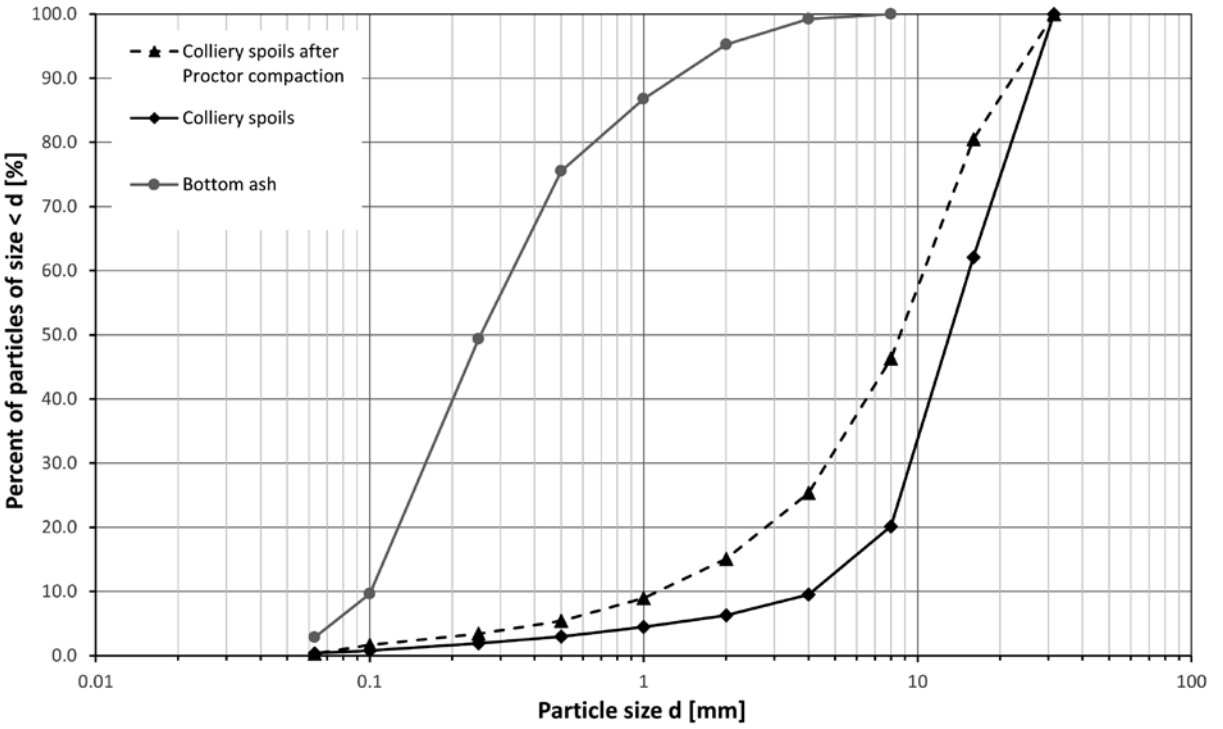


Text-fig. 1. Particle size distribution of the two raw materials analysed in the study.

imum particle size of the aggregate, 31.5 mm, was reduced by discarding the small proportion of grains larger than 15 mm that did not break apart easily when hit with a rubber hammer (colliery spoils are prone to grain disintegration, e.g., caused by compaction; see Text-fig. 1). As a result, the greatest particle size is approximately equal to 1/5 of the sample diameter. This procedure enabled testing in a standard-sized triaxial compression apparatus.

The mixture was prepared by adding dry bottom ash to water-saturated spoils with an extra amount of batch water, reaching the pre-assumed weight ratio (following Table 2). Mixing was done manually until apparent homogeneity. The ready mixture was immediately placed inside the test moulds, made of segments of a 75×3.0 mm PE-HD pipe with the bottom end blocked by a hardened gypsum grout plug. The compaction was done inside the moulds with a steel rammer (diameter 30 mm, weight 3.5 kg) in layers of c. 5 cm each, rammed 15 times from a height of c. 25 cm. The surface of the compacted layers was scarified before placing the next layer to achieve better adhesion.

The compacted test samples in moulds were wrapped and sealed in two layers of plastic and stored in a controlled environment at a temperature of 20 ± 1ºC. After 60 days of curing, the hardened samples were unsealed and cut to a desired length by a concrete-cutting saw; the plastic moulds were carefully cut open (Text-fig. 2).

The expected bulk density of the test mixture after compaction lies within the range of 1.66–1.68 g/cm$^3$, based on preliminary Proctor tests [rammer A, mould type B according to PN-EN 13286-2 (PKN 2010)]. The actual test samples prepared in two separate batches (same composition and preparation) differ in density (Table 3). This is most likely a result of an exceptional heterogeneity of the colliery spoils, consisting of several different minerals. Excess material from the cutting of the samples was tested for

| Batch | Number of samples | Mixture age during testing [days] | Bulk density of fresh mixture [g/cm$^3$] | | Water content after curing [%] | |
|---|---|---|---|---|---|---|
| | | | mean | SD | mean | SD |
| A | 6 | 60–70 | 1.63 | 0.019 | 14.6 | 1.2 |
| B | 15 | | 1.70 | 0.028 | | |

Table 3. Basic properties of mixture samples.

Text-fig. 2. Test sample with the plastic mould cut open (left) and basal surface of a test sample (right).

water content (oven-dried at 70ºC to a constant mass; Table 3). Some of these samples were tested as prepared, and another group was inundated for 36 h, reaching about 20–25% water content (this distinction is further described as the 'dry'/'wet' sample type, though no drying *per se* was done).

**Testing procedures and experiment schedule**

The central part of the experiment in terms of mechanical properties involved testing the hardened spoil-ash mixture samples in triaxial stress-strain conditions, i.e.,:

The bender element test (BET) was used to estimate the potential stiffness changes after wetting. This system can generate S- and P-wave types in the range of 0.5–100kHz, with an acquisition rate of 2 MHz. The focus here is on S-waves, as their velocity is not affected by the presence of water (degree of saturation) *per se*. However, it depends on the stress state and material structural stiffness, which may change due to shifts in water content. The methodology was initially introduced, among others, by Dyvik and Madhus (1985) and Viggiani and Atkinson (1995). The test is carried out on cylindrical samples placed into the triaxial testing chamber, where isotropic confining stress is applied, in this case: $\sigma_3$ = 0 kPa; 50 kPa; 200 kPa; 350 kPa; 500 kPa. Then, S-waves (shear waves) are generated and picked up along the vertical sample axis by a bender element mounted into the pedestal and top cap (Text-fig. 3). Wave velocity is calculated from the time of wave travel through the height of the sample. The small strain shear modulus $G_0$ is further derived as follows (Viggiani and Atkinson 1995):

$$G_0 = \rho \cdot V_s^2 = \rho \cdot \left( \frac{L^2}{t^2} \right) \qquad (1)$$

where: $\rho$ is the soil bulk density, $V_s$ is the shear wave velocity, $L$ is the effective sample length, and $t$ is the wave travel time.

The Appendix presents the test schedule. Due to the non-destructive character of the BET test, some

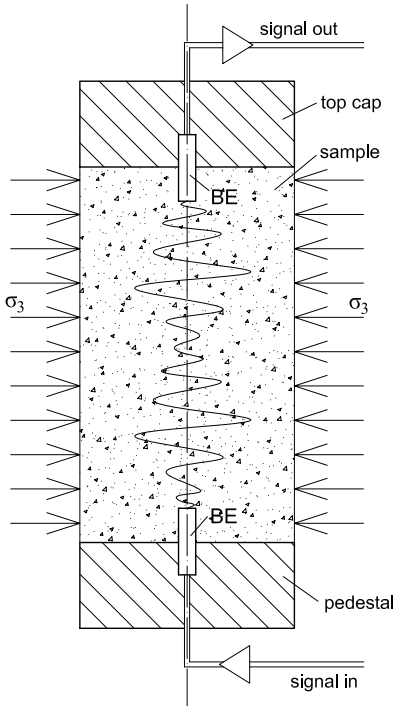


Text-fig. 3. Bender element test sample setup

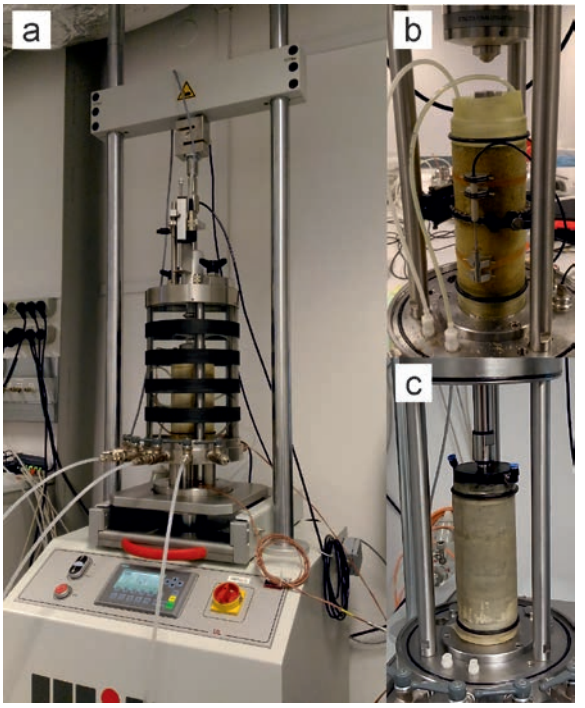


Text-fig. 4. Triaxial test setup. A – sample specimens in the triaxial cell; B – triaxial cell with local LVDT strain sensors; C – triaxial cell in basic setting.

of the 'dry' and 'wet' samples were used to further examine strength parameters in the triaxial compression test (TRX).

For shear strength characterization, four series of triaxial compression tests (TRX) were performed. Two series were performed on 'dry' samples, one under constant vertical strain rate of $v_{sh}$ = 0.2 mm/min, and the second under constant vertical stress rate of $v_{sh}$ = 60 kPa/min. Two other series with the same approach for loading variations were performed on the 'wet' samples. Loading rates were chosen based on regulations in the ASTM D 2664-95a (ASTM 1997) standard. The equipment used is shown in Text-fig. 4. Each test series (four to five samples) was sheared under different confining stresses in the range $\sigma_3$ = 0 kPa; 50 kPa; 200 kPa; 350 kPa; 500 kPa. The classic Coulomb-Mohr model was used to interpret the total stress-based angle of internal friction ($\varphi$) and cohesion ($c$). Tests were performed in UU configuration, allowing for pore pressure measurements and thus also effective stress analysis (ESA). Because the samples were not fully saturated (as inundation in water does not assure such a condition), those measurements may serve as an indicative measure rather than a precise reference. This intentional simplification of the procedure was, in our opinion, useful for making it similar to a common practical approach and real-life scenario.

Additionally, the matric suction (unsaturated soil theoretical background based on Fredlund and Rahardjo 1993) value assessment was needed for 'dry' samples to estimate its influence on apparent cohesion in triaxial test interpretation, and appropriate assessment of the effective stress for BET tests. Those measurements were performed using a self-developed device equipped with a ceramic needle positioned into pre-drilled holes in the samples after completion of BET and TRX measurements. The ceramic needle used has an air entry value at the level of 200 kPa. It was thoroughly de-aired and saturated together with a connecting tube in a vacuum chamber. After placement into the sample, each measurement took about 10–30 min. until reading stabilization. About 50 valid measurements were made, excluding those where cavitation occurred in the system. Text-fig. 5 shows elements of the suction measurement system during operation. The maximum matric suction measured was about -75 kPa, with an average of -68 kPa. From previous experiences of such measurements on different materials, we deduce that the measured values may be highly underestimated here. For accurate


Text-fig. 5. Suction measurement: readout unit (left), ceramic needle prepared for measurement (centre), ceramic needle inserted into a prepared hole during the measurement (right).

measurement, the ceramic needle surface needs to be in tight contact with the material, which seems practically impossible here. The needle could not be pushed into it, as is the case when testing softer soils; pre-drilled holes were used instead, but their shape inevitably did not ideally mirror the shape of the needle. Some fine ash was used to partly fill the hole and allow better coupling. Nevertheless, the actual matric suction values are probably considerably lower (more negative). The above mentioned mean value was used for calculating effective stress in TRX and BET tests for 'dry' conditions, as a conservative approach. In a future work we plan to try the usage of a more advanced axis translation technique (with direct monitoring of water and air pore pressure, which allows calculations of matric suction) to more precisely capture the effective stress path during the test, although it is unknown if this will be feasible, due to the challenges that this type of material presents. Namely the highest concern is whether it is possible to prepare the sample to ensure its perfectly flat bottom surface and to be in contact with high air entry porous disc, which is a critical condition for the reliable measurement of pore water pressure in unsaturated samples.

## RESULTS

### Stiffness characteristics (BET)

The first measurements of the shear wave velocity ($V_s$) were performed with no confining pressures in the triaxial cell. The aim was to estimate initial, 'dry' sample variability before inducing any further factors. The basic statistical parameters shown in Table 4 indicate a considerable scatter, which is probably a combined result of the aforementioned exceptional heterogeneity of colliery spoils and uncertainties in the BET measurements. Nevertheless, this initial reading is used later to calculate relative changes induced by further confining stress increments and wetting.

As an initial analysis, the relative change of $V_s$ after wetting is presented (Text-fig. 6). If a simple, common approach of total stress analysis (TSA) is used, a substantial decrease of $V_s$ (thus $G_0$) after wetting is observed. This relative change reaches 30% in some cases. On the other hand, when measured suction is considered, we may derive that effective stress acting on the 'dry' samples without any external confining stress being applied equals approximately 68 kPa (we have assumed the average value of matric suction as a reference value of pore pressure). Then, comparing $V_s$ measured in the 'dry' sample with $V_s$ estimated from the line of best fit for measurements of the inundated sample, it turns out that the relative change is as small as a few percent (except sample B3, but even here, reduction to half of the TSA-derived estimation is observed).

| | Shear wave velocity $V_S$ [m/s] |
|---|---|
| max | 404 |
| min | 230 |
| average | 325 |
| SD | 49 |

Table 4. $V_s$ scatter for initial (confining stress $\sigma 3$ = 0 kPa) 'dry' samples.

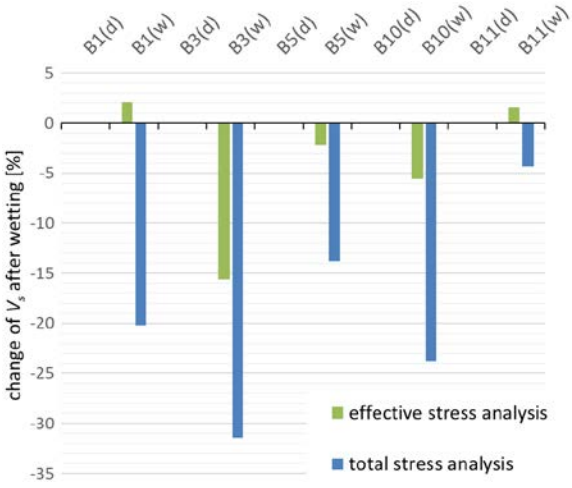


Text-fig. 6. Relative change of $V_s$ after wetting in percent (no confining stress applied), without correction for matric suction (total stress analysis) and after correction (effective stress analysis). B1–B11 indicate the tested samples.

Samples undergoing a series of confining stress stages of BET revealed the expected and well-known dependency of increasing stiffness (represented by the initial shear modulus $G_0$) with increasing stress value. 'Wet' samples showed similar trends, but their stiffness was reduced (Text-fig. 7).

The scale of this reduction varies significantly depending on whether matric suction is considered during the interpretation. This stiffness degradation of averaged $G_0$ value (represented by dotted lines on the graph) in relation to 'dry' samples' averaged $G_0$ (under the same confining stress) ranges from -9 to -41% for total stress and from -5 to -20 for effective stress (Text-fig. 8). It is important to mention that the bulk density used for $G_0$ calculation (in accordance with equation 1) was equal to 1.67 g/cm$^3$ for 'dry'

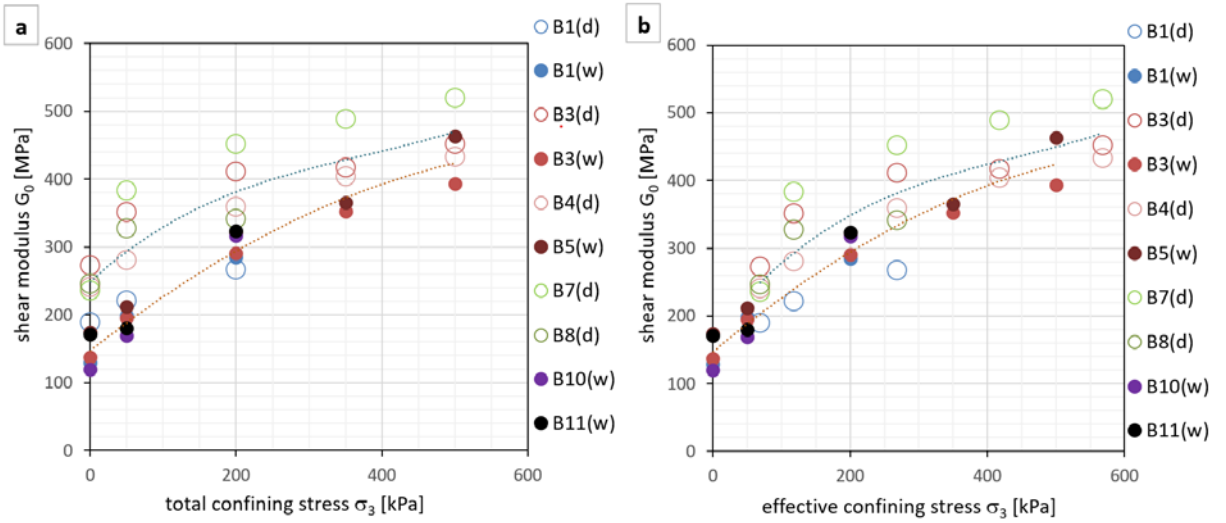


Text-fig. 7. Shear modulus $G_0$ (under different confining stress) on 'dry' samples (marked d) and subsequent results after wetting (marked w). A – total stress analysis; B – effective stress analysis. B1–B11 indicate the tested samples.

samples, and 1.78 g/cm$^3$ for 'wet' samples. This difference in bulk density (due to water content) further closes the gap between the $G_0$ results, compared to raw $V_s$ measurements.

## Strength characteristics (TRX)

TSA on 'dry' samples and under constant stress rate loading revealed the C-M model strength parameters at $\varphi = 35^o$ (angle of internal friction) and $c = 380$ kPa (apparent cohesion). Corresponding 'dry' samples sheared under constant strain rate loading conditions gave very similar results, i.e., $\varphi = 35^o$ and $c = 410$ kPa.

TSA for two series of 'wet' specimens suggests a significant material weakening. The angle of internal friction was reduced by ~17%; $\varphi = 29^o$, while apparent cohesion decreased by 58%; $c = 160$ kPa. In a series of tests using a constant strain rate, the angle of internal friction ($\varphi = 35^o$) remained unchanged. However, there was a nearly ten times decrease in apparent cohesion $c$ to a value of 40 kPa, compared to the results of 'dry' samples, sheared by the same method.

The same results can be interpreted with pore pressure influence (negative for 'dry' samples and positive for 'wet' samples) in ESA. As it was impossible to measure matric suction during shearing (with the particular equipment used), a constant average value of -68 kPa was used for correcting the calculated stress value of the 'dry' samples. 'Wet' samples were corrected for excess pore water pressure. Such an approach reduces the differences between maximum shear stress and cohesion for 'dry' and 'wet' samples, leaving values of the angle of internal friction relatively unchanged. For the stress rate test, the change in cohesion ranges from 260 to 200 kPa and, for the strain rate test, from 290 to 130 kPa. This gives a maximum of about a two-fold reduction instead of an almost ten-fold one (should the total stress interpretation be applied). Text-fig. 9 shows the graphical presentations of the above results in a Coulomb-Mohr en-

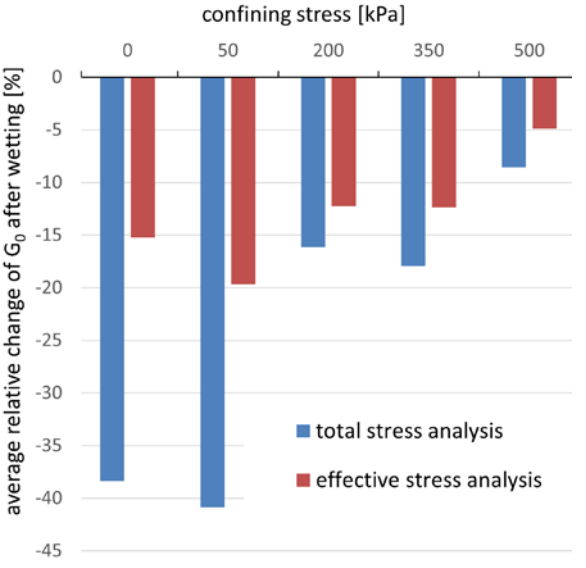


Text-fig. 8. Average relative changes of shear modulus $G_0$ after wetting for different values of confining stress, using total and effective stress interpretation.

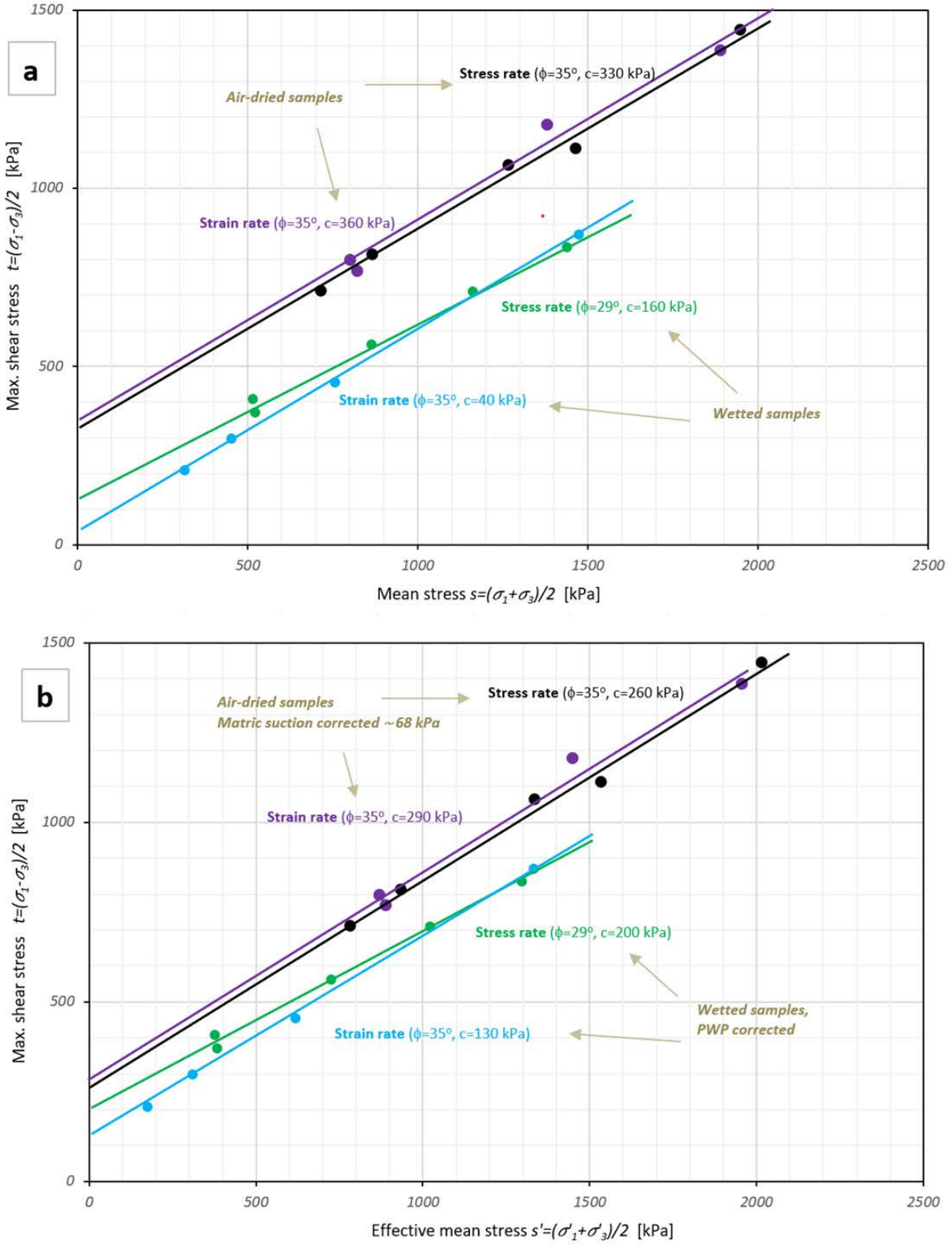


Text-fig. 9. Coulomb-Mohr failure envelopes in the *t-s* plane for all four series of triaxial compression tests, for A – total stress analysis, and B – effective stress analysis.

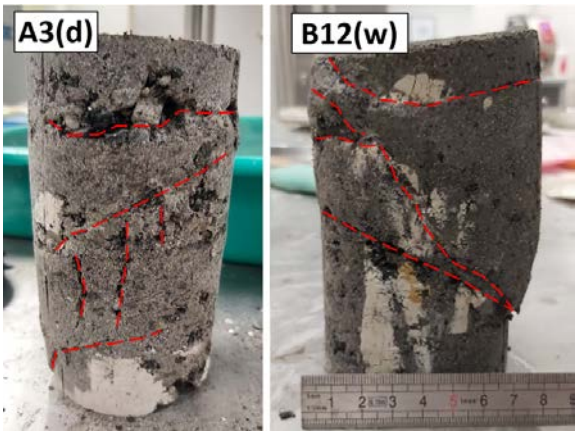


Text-fig. 10. Photographs showing samples A3(d) and B12(w) after shearing (thin red dashed lines indicate fractures).

velope in the *t-s* plane for both analytical approaches. It should be noted that this whole analysis is with the use of a very conservative assumption regarding excess pore water pressure and suction pressure (due to the reasons described earlier), and if those pressures are of a bigger scale, the apparent strength reduction would be even less pronounced.

The mode of loading (constant shear strain and constant stress rate) did not seem to have any influence on the results of 'dry' samples. With 'wet' samples, stress-controlled test results diverged most from those expected, as the angle of internal friction could be less affected by any real or apparent weakening after wetting. Nevertheless it is difficult to speculate, mainly due to the discussed uncertainties related to pore pressure distribution.

Regardless of the specimens' wetting, the failure nature remained brittle (Text-fig. 10), with shear reaching several percent of axial strain (0.6–6%).

### Matric suction measurements

Matric suction measurements have been performed on 'dry' samples after BET and TRX tests. Values obtained from about 50 reliable measurements ranged from -50 to -75 kPa, with a mean value of -68 kPa.

## DISCUSSION

### Interpretation of the test results

A general overview of the main results of all the tests can be found in Tables 5 and 6. Total and effective stress analysis give us different views on the soil characteristics. The question arises: which view is more appropriate, accurate, and safer.

From a practical engineering point of view, TSA directly answers how material characteristics (in this case, stiffness and strength parameters) change in response to a particular trigger (inundation of the material in water in this study). It is a useful approach as long as there is no shortcut in thinking that the trigger is the actual cause of the material response. In this case, when ESA is used (with all simplifications involved), it becomes evident that water changes the stress state conditions, and the material changes its

| Test method | | BET | | | | |
|---|---|---|---|---|---|---|
| Analysis type | Aample type | Conditions | Shear wave velocity $V_S$ | | Shear modulus $G_0$ | |
| | | | mean [m/s] | % change | mean [MPa] | % change |
| TSA | dry | no confining stress | 347 | – | 201 | – |
| | wet | | 268 | -22 | 119 | -40 |
| ESA | dry | effective stress 68 kPa | 353 | – | 208 | – |
| | wet | | 338 | -4 | 190 | -8 |

Table 5. Summary of triaxial compression (TRX) test results.

| Test method | | TRX | | | | | | | |
|---|---|---|---|---|---|---|---|---|---|
| Analysis type | Sample type | Angle of internal friction $\varphi$ – const. stress rate | | Angle of internal friction $\varphi$ – const. strain rate | | Cohesion $c$ – const. stress rate (apparent for TSA, effective for ESA) | | Cohesion $c$ – const. strain rate (apparent for TSA, effective for ESA) | |
| | | mean [°] | % change | mean [°] | % change | mean [kPa] | % change | mean [kPa] | % change |
| TSA | dry | 35 | – | 35 | – | 330 | – | 360 | – |
| | wet | 29 | -17 | 35 | 0 | 160 | -51 | 40 | -88 |
| ESA | dry | 35 | – | 35 | – | 260 | – | 290 | – |
| | wet | 29 | -17 | 35 | 0 | 200 | -23 | 130 | -55 |

Table 6. Summary of bender element (BET) test results.

behaviour accordingly, with regard to strain-stress fundamental principles. That does not fully explain the measured parameter degradation but reduces the scale of it by at least half or more. In other words, actual material weakening caused by some structural changes due to interaction with water is much smaller than it would appear from a TSA point of view. Moreover, the supposed limitations of the applied method underestimate the assumed suction values (as mentioned above under material and methods), and excess pore water pressure measured during shearing is not fully representative (underestimated due to the lack of full saturation). In that case, this apparent material degradation may be even smaller.

Differentiating between apparent and real material degradation is essential. Apparent changes are reversible with a change of stress state, while real material weakening will accumulate, and degradation may increase with further wetting-drying cycles, should they occur.

Some literature examples of the influence of material wetting on shear wave velocities (using the BET method) have been summarized with the following conclusions:

– partial saturation creates capillary forces between grains, enhancing particle contact and increasing small strain stiffness compared to dry material (Alramahi *et al.* 2008). Fully dried soil yields decreasing wave velocity, as the lack of capillary force disrupts particle bonding (Goertz and Knight 1998). In general, increasing capillary force in partially saturated soil is correlated with increasing S-wave velocity $V_s$, as well as shear modulus $G_0$ (Qian *et al.* 1993);
– after introducing initial amounts of pore water (less than 10% water saturation, fine sand samples), a further water content increases results in decreasing wave velocities due to increasing bulk density and diminishing capillary force. The change in $V_s$ is considerably more pronounced than in $V_p$ (Kim *et al.* 2021);
– the decreasing $V_s$ trend continues with saturation levels approaching 100% (Kim *et al.* 2021).

Obviously, these examples refer to cohesionless materials (sands), and as such, are not a direct comparison for this study. But they are cited here to show that it is actually the change in effective stress that the above authors are referring to (talking about changes in capillary forces), testing wave velocities, not material structural changes and their effect on $V_s$.

The shear strength test results from the TRX method correspond with some of the previously published papers (Zawisza and Gruchot 2017; Gruchot *et al.* 2020). A decrease of cohesion with increasing water content is not unique, and neither is the small change, or none, of the internal friction angle. The cited papers used TSA.

The question remains about the actual structure degradation mechanism, which seems to occur, although to a relatively limited extent. The interplay between the water content and the properties in natural soils includes many phenomena.

According to Feng *et al.* (2023), concerning their testing of red clay, $\varphi$ of soil depends mainly on the occlusion between grains, while $c$ is a result of cementation between particles. The interlocking behaviour is a product of grain structure, size, and soil density, all of which are not significantly affected by fluctuations in water content. An increasing water content translates to more capillary water but weakens the water film effect of bound water, thus diminishing the water film bonding force. Simultaneously, the adhesion effect between soil particles depends on their minerals, some of which may dissolve with increasing water supply, thus lowering the bonding force.

Besides the hypothesis above, which remains likely in relation to the spoil-ash mixtures, there are some additional considerations regarding this particular man-made soil. The colliery spoils are prone to grain disintegration under cycles of wetting-drying (Skarżyńska 1995a). They are also not chemically inert, for example, susceptible to microbially-induced pyrite oxidation (Bérubé *et al.* 1986). The not completely reacted FBC ash can hydrate and swell in contact with additional water (it contains anhydrite and lime); some of the minerals may also dissolve or lose strength (e.g., gypsum) or react with the constituents of colliery spoils. Some information on the chemical reactivity of spoils and ash can be found in Krysiak *et al.* (2023). These specific properties are likely to enhance the negative impact of sudden water intake on the geomechanical properties of the mixtures in the short term and after cyclic wetting-drying (not included in this experiment).

**The impact on the safety of structures**

Due to the availability of the material, colliery spoils and FBC bottom ash mixtures are mainly used as construction material for embankments. Therefore, as part of the study, it was decided to illustrate the impact of wetted material on the stability of embankment slopes. Laboratory tests proved that as a result of water saturation of the samples, there is some decrease in apparent cohesion from $c$ = 380 kPa in ‘dry’ conditions to $c$ = 40 kPa in ‘wet’ conditions when

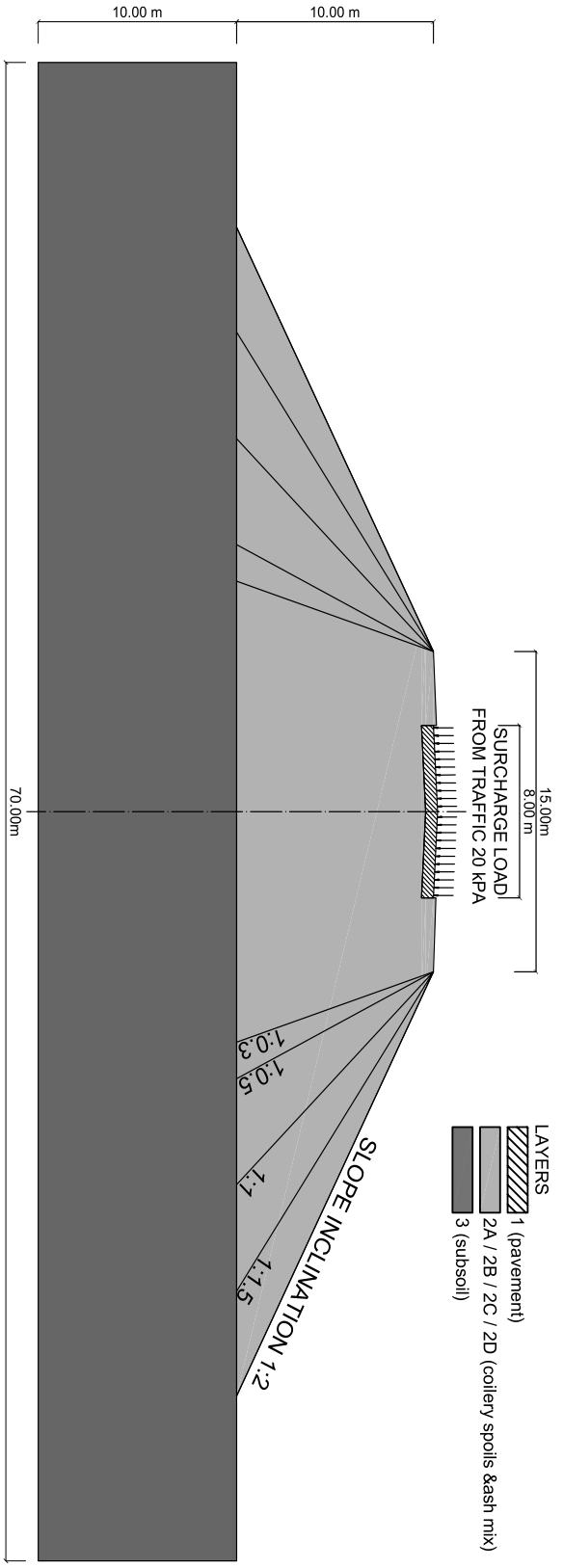


Text-fig. 11. Geometry of the FEM model with slope inclination variants.

using TSA, whereas the change was not as dramatic when ESA was utilized, with *c* attaining values from 290 kPa to 130 kPa. A reduction in the angle of internal friction also occurs, but it is a reduction of only a few degrees. Both parameters determine the shear strength, which directly impacts slope stability. All calculations were performed by the finite element method using ZSOIL (ver. 16.10) software. To evaluate the safety factor (SF), the strength parameter reduction method (phi-c reduction method) was used, more extensively described by Zimmermann *et al.* (1987), as well as Matsui and San (1992). Calculations were carried out for several models with varying slope inclinations to fully evaluate the impact of strength reduction caused by the wetting factor. The slope inclinations ranged from 1:0.3 to 1:2. 1:1.5 is an actual road embankment slope inclination made of the studied material. The model scheme is shown in Text-fig. 11. The pavement layer (layer 3) was modelled as an elastic material and loaded with 15 kPa as a typical surcharge load from traffic for embankments higher than 4 m in a 2D dimension problem (Topolnicki 2020) increased by 33% (+5 kPa) to cover road traffic dynamic effects.

The subsoil and the spoil-ash mixture layer were modelled using the Mohr-Coulomb model. The substrate layer was excluded from the parameter reduction during the phi-c reduction procedure. The parameters of the modelled layers are summarized in Table 7.

The safety factor calculations proved that stability will be preserved even for very steep slopes (SF>1) for both ‘dry’ and ‘wet’ conditions. However, the moisture content of the material causes some reduction in the stability reserve.

Regardless of the slope inclination, the safety factor reduction for ‘dry’ conditions and TSA parameters (range of SF from 9.9 to 18.3 depending on the slope angle) is about five times higher than for ‘wet’ conditions (range of SF from 1.6 to 3.3, respectively). This observation leads to the conclusion that the influence of material wetting has a significant negative effect on stability. The results based on effective parameters (ESA), which should be taken into account in the case of long-term stability analysis, do not confirm such a substantial reduction. There is also a difference between the stability results calculated based on ESA parameters in dry and wet conditions, but it is not as significant as in the case of the analysis using TSA parameters. In this case, there is only a double reduction in the safety factor and the safety reserve is two times higher in wet conditions than provided by the analysis based on TSA parameters.

| Layer no. | Layer type | Conditions | Unit weight $\gamma$ [kN/m$^3$] | Young modulus $E$ [MPa] | Poisson ratio $\nu$ [-] | Internal friction $\varphi$, $\varphi'$ [°] | Cohesion $c$, $c'$ [kPa] | Dilatancy angle $\Psi$ [°] | Material formulation |
|---|---|---|---|---|---|---|---|---|---|
| 1 | subsoil | – | 21.5 | 30 | 0.25 | 18 | 30 | 0 | M-C |
| 2A | colliery spoils and ash mix | wet | 18 | 154 | 0.4 | 29 | 40 | 4 | |
| 2B | | dry | 17 | 154 | 0.4 | 35 | 380 | 4 | |
| 2C | | wet | 18 | 154 | 0.4 | 35 | 130 | 4 | |
| 2D | | dry | 17 | 154 | 0.4 | 35 | 290 | 4 | |
| 3 | pavement | – | 22 | 800 | 0.3 | – | – | – | elastic |

Table 7. Summary of parameters assumed in the FEM model.

As part of the stability modelling, the minimum cohesion value for the equilibrium state SF = 1 was calculated (Text-fig. 12). This value was determined for all variants of the embankment slope assuming a constant value of the angle of internal friction at the minimal value determined in the presented research $\varphi$ = 29º. The cohesion values providing the equilibrium state are significantly lower than the cohesion reduced due to the action of water on the embankment material.

This does not change the fact that there is a reduction in the safety factor. This essential fact should be considered when designing the embankment's structural layers to isolate the material from rain and groundwater. The careful application of this material would be particularly vital in flood protection dikes, which are exposed to water seepage, temporary saturation, and drying while usually lacking a drainage system.

The results of the FEM calculations are summarized in Text-figs 12 and 13. In light of the evident unfavourable changes in the geomechanical properties of the spoil-ash mixtures caused by increase in the water content, consideration of further laboratory

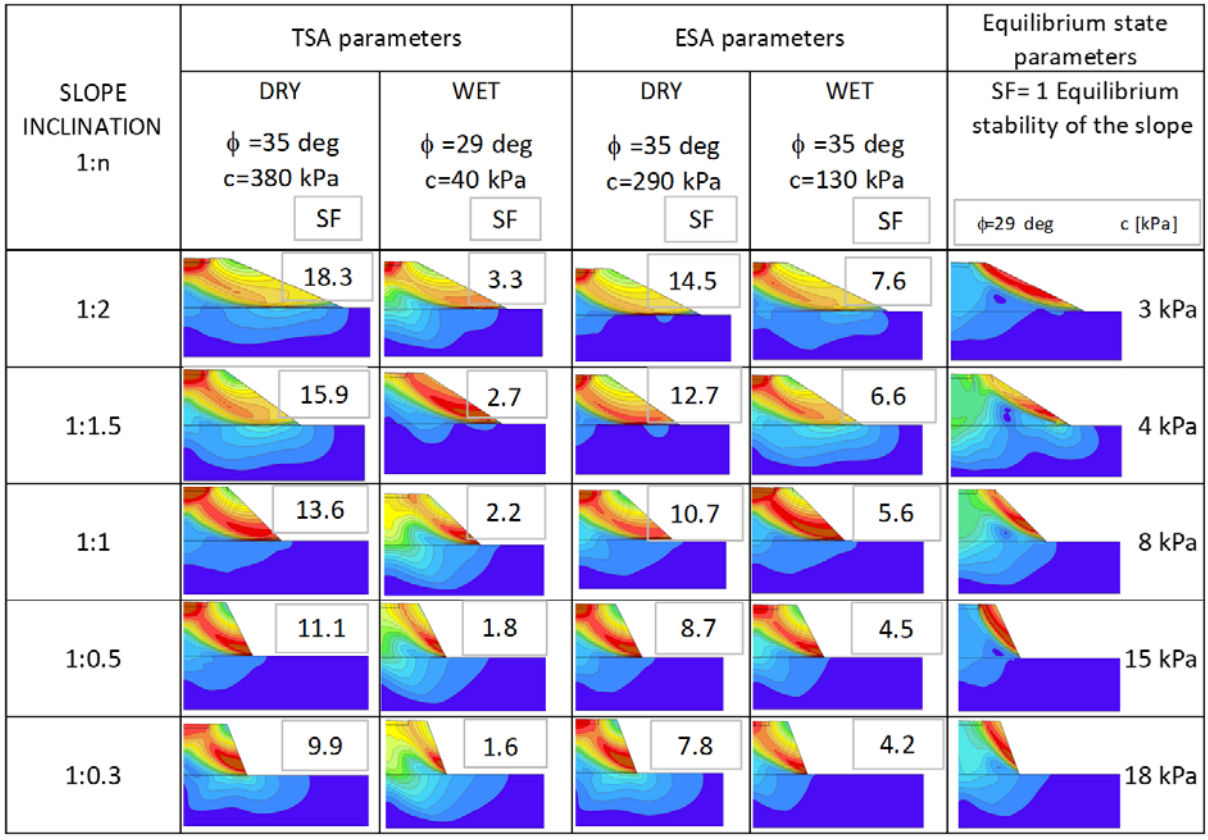


Text-fig. 12. Summary of slope stability test results from the FEM model, Safety Factors, and minimal cohesion in the equilibrium state shown to the right of images.

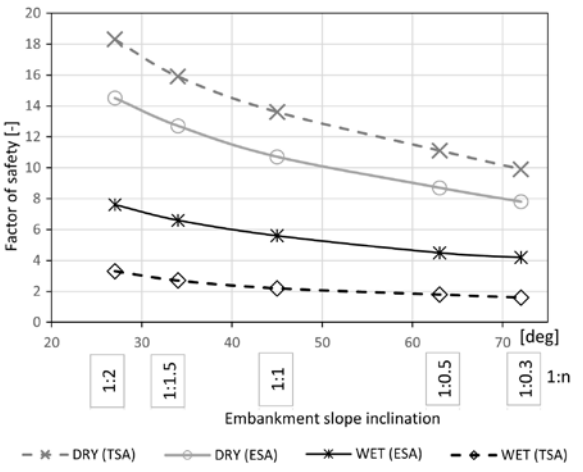


Text-fig. 13. Safety factor depending on the slope inclination for total stress (TSA) and effective stress (ESA) parameters for 'wet' and 'dry' samples.

tests seems reasonable, expanding on the results presented in this paper. Future analyses might consider multiple different saturation levels (including completely dry), extended inundation periods, reversibility of changes with more wetting-drying cycles, water filtration through material samples, etc.

## CONCLUSIONS

1. The tested samples of uniformly prepared colliery spoils and FBC ash bound mixture exhibit relatively high and stable angle of internal friction, in the range of 29–35º (TRX tests under variable strain-stress and wetting conditions).

2. Apparent cohesion *c*, on the other hand, was reduced while samples were subjected to inundation in water for 36 h before tests. The scale of this reduction depends on whether total or effective stress analysis is implemented, ranging from 380 kPa ('dry' samples) to 40 kPa ('wet' samples) for total stress and from 290 to 130 kPa for effective stress. This finding is consistent with the concept of effective stress in unsaturated soils, wherein matric suction increases the effective confining pressure, thereby maintaining higher strength/stiffness in the 'dry' state

3. Small strain stiffness, represented by initial shear modulus $G_0$, has been confirmed to diminish in BET tests by up to -41% after sample inundation judging by total stress and up to -20% including pore pressure changes (effective stress analysis). This reduction in $G_0$ is lower as the confining stress value increases.

4. The approach using total stress analysis is common due to the simplicity of test methods and interpretation. It is a valid design tool, practical and robust, referring to externally observed changes in material behaviour. However, judging from a research perspective, it hugely limits our understanding and capability to separate cause from effect or blurs the reference used for comparisons.

5. The possible causes of the material degradation after inundation may include dissolution or reaction of minerals and grain disintegration after wetting. The latter two are typical for the material under investigation and other similar man-made soils. The presented research does not allow for the establishment of the primary cause, but it suggests that the spoil-ash mixture is no more prone to this kind of degradation than natural soils described in the cited studies.

6. Slope stability analysis of examples shows that with an embankment height of 10 m, even the lowest obtained strength parameters would provide enough safety margin with the steepest slopes (SF no less than 1.6). Still, the reduction in safety factors in 'wet' material relative to 'dry' material embankment is considerable, c. five-fold (TSA) or c. two-fold (ESA). Total stress analysis yields underestimated Safety Factors in the 'wet' state.

7. The results indicate the need for a detailed analysis of the use of the specific material in the context of the planned loads and water conditions. In addition to the strength characteristics of the particular material, which belongs to an important group of industrial by-products used in engineering, the performed research provides universal methodological conclusions.

All relevant data and models generated or used during the study are stored in Mendeley Data scientific repository under DOI: doi.org/10.17632/8xfppn9j5j.2.

**Acknowledgements**

We would like to thank the Head of the Laboratory of Applied Geology at the Faculty of Geology, University of Warsaw for granting access to perform the BET and suction measurements. We gratefully acknowledge the valuable feedback provided by the reviewers and believe that it has contributed to enhancing the scientific rigor and overall presentation of this work.

## REFERENCES

Alramahi, B., Alshibli, K.A., Fratta, D. and Trautwein, S. 2008. A suction-control apparatus for the measurement of P and

S-wave velocity in soils. *Geotechnical Testing Journal*, **31**, 12–23.

ASTM 1997. ASTM D2664-95a Standard Test Method for Triaxial Compressive Strength of Undrained Rock Core Specimens Without Pore Pressure Measurements. ASTM Annual Book of Standards. Available at: https://doi.org/10.1520/D2664-95A.

Babets, D.V., Kovrov, O.S., Moldabayev, S.K., Tereschuk, R.M. and Sosna, D.O. 2020. Impact of water saturation effect on sedimentary rocks strength properties. *Naukovyi Visnyk Natslionalnoho Hirnychoho Universytetu*, **2020** (4), 76–81.

Bérubé, M.-A., Locat, J., Gélinas, P., Chagnon, J.-Y. and Lefrançois, P. 1986. Black shale heaving at Sainte-Foy, Quebec. *Canadian Journal of Earth Sciences*, **23**, 1774–1781.

Bisht, A. 2022. Sand futures: Post-growth alternatives for mineral aggregate consumption and distribution in the global south. *Ecological Economics*, **191**, 107233.

Borys, M., Mosiej, K., Czartoryski, J. and Filipowicz, P. 2002. Wytyczne stosowania odpadów pogórniczych z kopalni Bogdanka do budowy wałów przeciwpowodziowych i innych budowli hydrotechnicznych, 68 pp. IMUZ; Falenty.

Cadierno, J.F., Romero, M.I.G., Valdés, A.J., del Pozo, J.M., González, J.G., Robles, D.R. and Espinosa, J.V. 2014. Characterization of colliery spoils in León: Potential uses in rural infrastructures. *Geotechnical and Geological Engineering*, **32**, 439–452.

Dyvik, R. and Madshus, C. 1985. Lab measurements of Gmax using bender elements. In: Koshla, V. (Ed.), Proceedings ASCE Annual Convention, Advances in the Art of Testing Soils under Cyclic Conditions, 186–197. American Society of Civil Engineering; Detroit.

CEN, 2004. EN 13286-50: 2004, Unbound and Hydraulically Bound Mixtures – Part 50: Method for the Manufacture of Test Specimens of Hydraulically Bound Mixtures Using Proctor Equipment or Vibrating Table Compaction. European Committee for Standardization; Brussels.

Feng, X., Teng, J. and Wang, H. 2023. Influence Mechanism of Water Content and Compaction Degree on Shear Strength of Red Clay with High Liquid Limit. *Materials (Basel)*, **17**, 162.

Fredlund, D.G. and Rahardjo, H. 1993. Soil mechanics for unsaturated soils, 517 pp. John Wiley & Sons; New York.

Gabryś, K., Šadzevičius, R., Dapkienė, M., Ramukevičius, D. and Sas, W. 2023. Effect of a Fine Fraction on Dynamic Properties of Recycled Concrete Aggregate as a Special Anthropogenic Soil. *Materials (Basel)*, **16**, 4986.

Gazdič, D., Fridrichová, M., Kulísek, K. and Vehovská, L. 2017. The potential use of the FBC ash for the preparation of blended cements. *Procedia Engineering*, **180**, 1298–1305.

Głuchowski, A., Gabryś, K., Soból, E., Šadzevičius, R. and Sas, W. 2020. Geotechnical properties of anthropogenic soils in road engineering. *Sustainability*, **12**, 4843.

Goertz, D. and Knight, R. 1998. Elastic wave velocities during evaporative drying. *Geophysics*, **63**, 171–183.

Gong, W., Quan, C., Li, X., Wang, L. and Zhao, C. 2022. Statistical analysis on the relationship between shear strength and water saturation of cohesive soils. *Bulletin of Engineering Geology and the Environment*, **81**, 337.

Gruchot, A. 2014. Utilization of post coal waste composites and fly ash for levee construction. *Przegląd Górniczy*, **70** (7), 158–164. [In Polish with English abstract]

Gruchot, A. and Zydroń, T. 2019. Shear strength of industrial wastes and their mixtures and stability of embankments made of these materials. *Applied Sciences*, **10**, 250.

Gruchot, A., Zydroń, T. and Michalska, A. 2020. The Influence of Compaction and Water Conditions on Shear Strength and Friction Resistance between Geotextiles and Ash-Slag Mixture. *Energies*, **13**, 1086.

IBDiM, 2010. Technical Approval AT/2010-02-2663. Mieszanka stabilizowana kruszywowo-popiołowa PKEW. {???}

Jafari, S.H. and Lajevardi, S.H. 2022. Influence of freeze-thaw cycles on strength and small strain shear modulus of fine-grained soils stabilized with nano-$SiO_2$ and lime using bender element tests. *Bulletin of Engineering Geology and the Environment*, **81**, 234.

Kettle, R.J. 1983. The improvement of colliery spoil. *Quarterly Journal of Engineering Geology*, **16**, 221–229.

Kim, J., Won, J. and Park, J. 2021. Effects of water saturation and distribution on small-strain stiffness. *Journal of Applied Geophysics*, **186**, 104278.

Kozioł, W. and Baic, I. 2019. Extraction, Production and Consumption of Gravel and Sand Aggregates in Poland An Attempt to Assess National and Regional Balances. *IOP Conference Series: Materials Science and Engineering*, **641**, 012033.

Krysiak, Ł. 2022. The impact of composition and loading on the swelling of mixtures of unburnt colliery spoils and fluidized bed bottom ash, 1–299. Unpublished PhD Thesis, Warsaw University of Technology, Warszawa. [In Polish with English abstract]

Krysiak, Ł., Kledyński, Z. and Machowska, A. 2023. Mixtures of colliery spoils and fluidized bed bottom ash: strength and swelling behavior under compressive stress in isolated conditions. *Bulletin of Engineering Geology and the Environment*, **82**, 164.

Laan, G., Van Westen, J.M. and Batterink, L. 1984. Minestone in hydraulic engineering application, deterioration and quality control. In: Symposium on the Reclamation, Treatment and Utilisation of Coal Mining Wastes, 5.1–5.10. Durham, England.

Matsui, T. and San, K.-C. 1992. Finite element slope stability analysis by shear strength reduction technique. *Soils and Foundations*, **32**, 59–70.

Mouazen, A.M., Ramon, H. and De Baerdemaeker, J. 2002. SW – Soil and water: Effects of bulk density and moisture con-

tent on selected mechanical properties of sandy loam soil. *Biosystems Engineering*, **83**, 217–224.

Ohenoja, K., Pesonen, J., Yliniemi, J. and Illikainen, M. 2020. Utilization of fly ashes from fluidized bed combustion: A review. *Sustainability*, **12**, 2988.

Pilecka, E. and Morman, J. 2017. Utilization of fine-grained mining waste strengthened cement for the modernization of flood embankments. *Zeszyty Naukowe Instytutu Gospodarki Surowcami Mineralnymi i Energią PAN*, **101**, 347–359. [In Polish with English abstract]

PKN 2022. PN-EN 1097-6:2022-07. Tests for mechanical and physical properties of aggregates – Part 6: Determination of particle density and water absorption. 63 pp. Polish Committee for Standardization; Warszawa.

PKN 2017. PN-EN ISO 17892-4:2017-01. Geotechnical investigation and testing – Laboratory testing of soil – Part 4: Determination of particle size distribution, 44 pp. Polish Committee for Standardization; Warszawa.

PKN 2010. PN-EN 13286-2:2010. Unbound and hydraulically bound mixtures – Part 2: Test methods for laboratory reference density and water content – Proctor compaction, 29 pp. Polish Committee for Standardization; Warszawa.

PKN 2008. PN-EN 1097-7:2008. Tests for mechanical and physical properties of aggregates – Part 7: Determination of the particle density of filler – Pyknometer method, 13 pp. Polish Committee for Standardization; Warszawa.

PKN 1988. PN-B-04481:1988 Grunty budowlane – Badania próbek gruntu, 63 pp. Polish Committee for Standardization; Warszawa.

Qian, X., Gray, D.H. and Woods, R.D. 1993. Voids and granulometry: effects on shear modulus of unsaturated sands. *Journal of Geotechnical Engineering*, **119**, 295–314.

Rainbow, A.K.M., Inz, H. and Skarzyńska, K.M. 1987. Minestone impoundment dams for fluid fly ash storage. *Advances in Mining Science and Technology*, **2**, 219–238.

Rajaram, G. and Erbach, D.C. 1997. Hysteresis in soil mechanical behavior. *Journal of Terramechanics*, **34**, 251–259.

Skarżyńska, K.M. 1995a. Reuse of coal mining wastes in civil engineering – Part 1: Properties of minestone. *Waste Management*, **15**, 3–42.

Skarżyńska, K.M. 1995b. Reuse of coal mining wastes in civil engineering – Part 2: Utilization of minestone. *Waste Management*, **15**, 83–126.

Suescum-Morales, D., Romero-Esquinas, Á., Fernández-Ledesma, E., Fernández, J.M. and Jiménez, J.R. 2019. Feasible use of colliery spoils as subbase layer for low-traffic roads. *Construction and Building Materials*, **229**, 116910.

Szymkiewicz, A., Hycnar, J.J., Fraś, A., Przystaś, R., Józefiak, T. and Baic, I. 2012. Application of fluidized bed combustion ashes for enhancement of mining waste management. *Inżynieria Mineralna*, **13** (1), 19–30.

Topolnicki, M. 2020. Road traffic loads for geotechnical analyses of embankments. *Ground Engineering*, **2020**, 1–10.

Viggiani, G. and Atkinson, J.H. 1995. Interpretation of bender element tests. *Geotechnique,* **45**, 149–154.

Wei, Y., Wu, X., Xia, J., Miller, G.A., Cai, C., Guo, Z. and Hassanikhah, A. 2019. The effect of water content on the shear strength characteristics of granitic soils in South China. *Soil and Tillage Research*, **187**, 50–59.

Yoon, S., Balunaini, U. and Prezzi, M. 2007. Forensic examination of severe heaving of embankment constructed with fluidized bed combustion ash. *Transportation Research Record*, **2026**, 9–17.

Zahedi, M. and Rajabipour, F. 2019. Fluidized Bed Combustion (FBC) fly ash and its performance in concrete. *ACI Materials Journal*, **116**, 163–172.

Zawisza, E. and Gruchot, A. 2017. Shear strength and bearing capacity of the ash-slag mixture aggregate depending on the water conditions. *Acta Scientiarum Polonorum. Formatio Circumiectus*, **16**, 13.

Zimmermann, T., Rodriguez, C. and Dendrou, B. 1987. Z_SOIL. PC: A program for solving soil mechanics problems on a personal computer using plasticity theory, In: Swoboda, G. (Ed.), Proceedings of the Sixth International Conference on Numerical Methods in Geomechanics, Austria, 11–15 April, Innsbruck, 2121–2126. Balkema; Rotterdam, Brookfield.

*Manuscript submitted: 15th July 2025*
*Revised version accepted: 20th October 2025*

# Appendix

Detailed experiment schedule; a – TRX, triaxial compression test; b – BET, bender element test.

| No. | Sample reference | 'dry' (d) / 'wet' (w) | TRX[a] test | BET[b] test | Confining stress (kPa; BET) | | | | |
|---|---|---|---|---|---|---|---|---|---|
| | | | | | 0 | 50 | 200 | 350 | 500 |
| 1 | A1 | d | + | – | – | – | – | – | – |
| 2 | A2 | d | + | – | – | – | – | – | – |
| 3 | A3 | d | + | – | – | – | – | – | – |
| 4 | A4 | d | + | – | – | – | – | – | – |
| 5 | A5 | d | + | – | – | – | – | – | – |
| 6 | A6 | d | + | – | – | – | – | – | – |
| 7 | B1 | d | – | + | + | + | + | – | – |
| 8 | | w | – | + | + | + | + | – | – |
| 9 | B2 | d | – | + | + | – | – | – | – |
| 10 | | w | + | – | – | – | – | – | – |
| 11 | B3 | d | – | + | + | + | + | + | + |
| 12 | | w | + | + | + | + | + | + | + |
| 13 | B4 | d | + | + | + | + | + | + | + |
| 14 | B5 | d | – | + | + | – | – | – | – |
| 15 | | w | + | + | + | + | + | + | + |
| 16 | B6 | d | – | + | + | – | – | – | – |
| 17 | | w | + | – | – | – | – | – | – |
| 18 | B7 | d | – | + | + | + | + | + | + |
| 19 | B8 | d | + | + | + | + | + | – | – |
| 20 | B9 | d | + | + | + | – | – | – | – |
| 21 | B10 | d | – | + | + | – | – | – | – |
| 22 | | w | + | + | + | + | + | – | – |
| 23 | B11 | d | – | + | + | – | – | – | – |
| 24 | | w | + | + | + | + | + | – | – |
| 25 | B12 | d | – | + | + | – | – | – | – |
| 26 | | w | + | + | + | – | – | – | – |
| 27 | B13 | d | – | + | + | – | – | – | – |
| 28 | | w | + | + | + | – | – | – | – |
| 29 | B14 | d | – | + | + | – | – | – | – |
| 30 | | w | + | + | + | + | – | – | – |
| 31 | B15 | d | – | + | + | – | – | – | – |